Acta Crystallographica Section F
Structural Biology and Crystallization Communications
ISSN 1744-3091

Crystallization and preliminary crystallographic analysis of β-mannanase from *Bacillus licheniformis*

Chomphunuch Songsiriritthigul,[a]* Sasithorn Lapboonrueng,[b] Sittiruk Roytrakul,[c] Dietmar Haltrich[d] and Montarop Yamabhai[b]

[a]Synchrotron Light Research Institute, 111 University Avenue, Nakhon Ratchasima 30000, Thailand, [b]School of Biotechnology, Suranaree University of Technology, 111 University Avenue, Nakhon Ratchasima 30000, Thailand, [c]Genome Institute, National Center for Genetic Engineering and Biotechnology, Pathumthani 12120, Thailand, and [d]BOKU, University of Natural Resources and Applied Life Sciences, A-1180 Vienna, Austria

Correspondence e-mail: chomphunuch@slri.or.th

Received 9 July 2010
Accepted 23 November 2010

The mannan endo-1,4-β-mannosidase (ManB) from *Bacillus licheniformis* strain DSM13 was overexpressed in *Escherichia coli*. Purification of the thermostable and alkali-stable recombinant mannanase yielded approximately 50 mg enzyme per litre of culture. Crystals were grown by hanging-drop vapour diffusion using a precipitant solution consisting of 12%(*w*/*v*) PEG 8000, 0.2 *M* magnesium acetate tetrahydrate and 0.1 *M* MES pH 6.5. The protein crystallized in the monoclinic space group $P2_1$, with two molecules per asymmetric unit and unit-cell parameters a = 48.58, b = 91.75, c = 89.55 Å, β = 98.29°, and showed diffraction to 2.3 Å resolution.

1. Introduction

β-Mannanase (endo-1,4-β-mannanase; mannan endo-1,4-β-mannosidase; EC 3.2.1.78) is an enzyme that catalyzes random hydrolysis of β-1,4-mannosidic linkages in the main chain of mannan and heteromannan (McCleary, 1988), which are abundant polysaccharides that are mainly found in plant seeds and plant cell wall (Moreira & Filho, 2008). β-Mannanases have drawn much interest because of their important roles in degrading mannan-containing polysaccharides; thus, various applications in the feed/food, pulp/paper and detergent industries have been reported (Dhawan & Kaur, 2007).

β-Mannanases belong to glycosyl hydrolase (GH) families 5 and 26 based on sequence-homology and hydrophobic cluster analysis (Henrissat, 1991; Henrissat & Davies, 1997). Both enzyme families cleave glycosidic bonds by a double-displacement mechanism that leads to retention of their anomeric configuration (Koshland, 1953; Harjunp *et al.*, 1995; Bolam *et al.*, 1996). Based on published three-dimensional structures (Hilge *et al.*, 1998; Sabini *et al.*, 2000; Hogg *et al.*, 2001; Ducros *et al.*, 2002; Akita *et al.*, 2004; Bourgault *et al.*, 2005; Le Nours *et al.*, 2005; Larsson *et al.*, 2006; Yan *et al.*, 2008), GH family 5 and GH family 26 mannanases both contain a characteristic core $(\beta/\alpha)_8$-barrel catalytic module.

Amino-acid sequence analysis revealed that the β-mannanase from *Bacillus licheniformis* (ManB) belongs to GH family 26 according to the CAZy (Carbohydrate-Active Enzymes) database (Cantarel *et al.*, 2009). Its sequence identities to other GH family 26 members of known structure are 15.43, 19.90 and 81.90% to *Cellulomonas fimi* mannanase (Le Nours *et al.*, 2005), *Pseudomonas cellulosa* mannanase (Hogg *et al.*, 2001; Ducros *et al.*, 2002) and *B. subtilis* Z-2 mannanase (Yan *et al.*, 2008), respectively. Generally, two catalytic glutamates are located at the ends of β-strands 4 and 7 of the C-terminal catalytic domain. Two solvent-exposed tryptophan residues (Trp172 and Trp298 in *B. subtilis* Z-2 mannanase; Yan *et al.*, 2008) are conserved throughout GH family 26 and play a crucial role in binding and catalysis. Structural and functional studies have indicated that the binding of Zn to a His-Glu-His motif within *B. subtilis* Z-2 mannanase contributes to its thermal stability.

B. licheniformis DSM13 was selected as a nonpathogenic host strain for isolation of the enzyme as this bacterium is very important in the biotechnology industry; it has been used extensively for large-

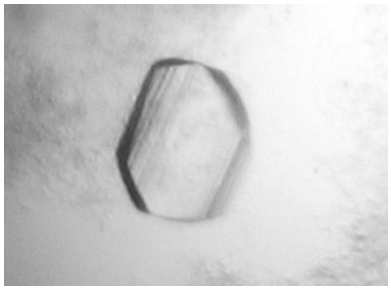

scale industrial production of many exoenzymes such as subtilisins, amylases and the antibiotic bacitracin (Schallmey *et al.*, 2004). The genome of this bacterium has recently been sequenced and revealed many new genes that are of potential interest for biotechnological applications, including one encoding a mannanase (Veith *et al.*, 2004).

B. licheniformis ManB is a relatively thermostable and alkali-stable β-mannanase that shows highest relative activity for glucomannan prepared from konjac, followed by pure low-molecular-mass 1,4-β-D-mannan of DP (degree of polymerization) <15 and high-viscosity (high-molecular-mass) locust bean gum (Songsiriritthigul, Buranabanyat *et al.*, 2010). TLC analysis of the hydrolysis products confirmed that recombinant *B. licheniformis* β-mannanase is an endo-mannanase which can efficiently and randomly cleave higher molecular-weight mannans consisting of more than six mannose monomers. In the present study, a large-scale purification of recombinant β-mannanase from *B. licheniformis* expressed in *Escherichia coli* was performed. The first crystal of β-mannanase from *B. licheniformis* and a preliminary analysis of its diffraction data are reported here. We aim to obtain the three-dimensional X-ray structure of the β-mannanase enzyme from *B. licheniformis* DSM13, which will be beneficial for understanding this enzyme and its application for the bioconversion of mannan into a commercially usable form of manno-oligosaccharide.

2. Materials and methods

2.1. Expression and purification of recombinant *B. licheniformis* β-mannanase

The *manB* gene from *B. licheniformis* (NCBI accession No. NC006322; bases 70–1080) was cloned into the *Bgl*II site of the pFLAG-CTS expression vector as described previously (Songsiriritthigul, Buranabanyat *et al.*, 2010). This fuses the enzyme to the *E. coli* OmpA signal sequence at the N-terminus and a hexahistidine tag at the C-terminus. The use of the *Bgl*II site adds two extra amino acids, arginine and serine, between the signal peptide and the mature enzyme. This expression system has been shown to be highly efficient for various extracellular hydrolytic enzymes such as mannanase and chitinase from *B. licheniformis* strain DSM13 (Yamabhai *et al.*, 2008; Songsiriritthigul *et al.*, 2009; Songsiriritthigul, Buranabanyat *et al.*, 2010; Songsiriritthigul, Lapboonrueng *et al.*, 2010).

The expression plasmid was transformed into *E. coli* Top10 (Invitrogen, Carlsbad, California, USA) and we found that this strain of *E. coli* is suitable not only for the cloning but also for the expression of various hydrolytic enzymes (Yamabhai *et al.*, 2011). The cells harbouring the mannanase gene were grown at 310 K in Luria–Bertani medium containing 100 mg l^{-1} ampicillin. Enzyme expression was induced by the addition of isopropyl β-D-1-thiogalactopyranoside (IPTG) to a final concentration of 1 m*M* when the OD_{600} of the cell culture reached ~1.0–1.5. Cell growth was continued at 298 K for 4 h and the cell pellet was collected by centrifugation at 4500*g* for 30 min. The freshly prepared cell pellet was resuspended in 10 ml lysis buffer [20 m*M* Tris–HCl buffer pH 8.0 containing 150 m*M* NaCl, 1 m*M* phenylmethylsulfonyl fluoride (PMSF) and 1 mg ml^{-1} lysozyme] and then lysed on ice using an Ultrasonic Processor with amplitude 60, pulser 6 s for 2 min. Unbroken cells and cell debris were removed by centrifugation at 12 000*g* for 45 min. The supernatant was applied onto an Ni–NTA agarose affinity column (1.0 × 10 cm; Qiagen GmbH, Hilden, Germany) and chromatography was carried out gravitationally following the manufacturer's protocol. After loading, the column was washed with 100 ml 20 m*M* Tris–HCl buffer pH 8.0, 150 m*M* NaCl containing 5 m*M* imidazole followed by another 50 ml of the same buffer containing 20 m*M* imidazole. 10 ml purified mannanase eluted with 250 m*M* imidazole was buffer-exchanged with 10 m*M* Tris–HCl buffer pH 8.0 and concentrated using Vivaspin-20 ultrafiltration membrane concentrators (10 kDa molecular-weight cutoff; Vivascience AG, Hanover, Germany). The protein solution was filtered through an Ultrafree-MC 0.22 µm filter (Millipore, Billerica, Massachusetts, USA) at 4000*g* for 10 min to eliminate dust and precipitated protein. Protein at a concentration of 20 mg ml^{-1} was stored in 10 m*M* Tris–HCl buffer pH 8.0 until use for crystallization purposes. Protein concentrations were determined by the method of Bradford (1976) using a standard calibration curve constructed from BSA (0–10 mg). The purity of the mannanase was verified by SDS–PAGE using a Laemmli buffer system (Laemmli, 1970).

A zymogram of mannanase activity was generated by an in-gel activity assay using 1%(*w*/*v*) locust bean gum as substrate copolymerized with 12%(*w*/*v*) polyacrylamide. The purified enzyme (1.7 ng) was electrophoresed according to a previously published protocol (Songsiriritthigul, Buranabanyat *et al.*, 2010). Mannanase activity was detected as a clear zone.

2.2. Crystallization

Initial crystallization experiments were carried out using the microbatch method in 60-well flat-bottom microwell plates (Nordic-Cell, Nunc, Copenhagen, Denmark) filled with 5 µl mineral oil containing vitamin E (BabyMild) following the previously published protocol (Chitnumsub *et al.*, 2004). For each crystallization drop, 1 µl enzyme solution (10 and 20 mg ml^{-1} in 10 m*M* Tris–HCl buffer pH 8.0) was added to 1 µl of each precipitant from Crystal Screen and Crystal Screen 2 (Hampton Research, Aliso Viejo, California, USA) and then incubated at 291 K. After 4 d incubation, needle clusters were obtained in condition 1 of Crystal Screen using 10 mg ml^{-1} mannanase. After incubation for 4 d, plate-shaped crystals were also produced in condition 13 of Crystal Screen 2 using 10 mg ml^{-1} enzyme. After 6 d incubation, needle clusters could also be observed in condition 15 of Crystal Screen using 20 mg ml^{-1} mannanase, whereas plate-like crystals were also obtained in condition 37 of Crystal Screen using 10 mg ml^{-1} protein. Plates were obtained after 10 d incubation in conditions 6 and 18 of Crystal Screen.

Conditions 15 and 18 of Crystal Screen and condition 13 of Crystal Screen 2 were further optimized using the hanging-drop vapour-diffusion method in 24-well VDX plates with sealant (Hampton Research, Aliso Viejo, California, USA). Protein drops were made up of 1 µl protein solution (3, 6 and 10 mg ml^{-1} in 10 m*M* Tris–HCl pH 8.0) mixed with 1 µl of various precipitants with varied precipitant and additive concentrations and pH and/or buffer type. Drops were equilibrated over 1 ml of the respective precipitant. For condition 18 crystals appeared in 12%(*w*/*v*) PEG 8000, 0.2 *M* magnesium acetate tetrahydrate in 0.1 *M* MES pH 6.5 within one week of incubation. Using protein concentrations of both 3 and 6 mg ml^{-1}, crystals with average dimensions of 160 × 115 × 15 µm were obtained. For condition 15 plates were obtained using 5 mg ml^{-1} protein sample and a precipitant solution consisting of 16%(*w*/*v*) PEG 8000, 0.2 *M* ammonium sulfate in 0.1 *M* MOPS pH 7.0. For condition 13 crystal clusters were produced in the conditions tested. Therefore, streak-seeding with a 10 000-fold dilution of crushed crystal clusters into pre-equilibrated drops made up of 2 mg ml^{-1} protein sample and precipitant consisting of 14%(*w*/*v*) PME 2000, 0.096 *M* ammonium sulfate in 0.1 *M* MES pH 5.5 was performed to generate single crystals.

2.3. Data collection

Before data collection, 5–25%(*v*/*v*) glycerol was added to the precipitant solution to optimize cryoprotection. The crystals optimized from condition 18 were briefly soaked in a cryoprotectant solution [25%(*v*/*v*) glycerol, 12%(*w*/*v*) PEG 8000, 0.2 *M* magnesium acetate tetrahydrate in 0.1 *M* MES pH 6.5], picked up in a nylon loop and quickly vitrified in a stream of nitrogen gas at 100 K. Diffraction images were collected on a MAR165 CCD detector system (MAR Research GmbH, Hamburg, Germany) mounted on a Microstar rotating-anode X-ray generator (Bruker GmbH, Karlsruhe, Germany) operating at 45 kV and 60 mA. The crystal-to-detector distance was set to 90 mm, with all frames collected at 100 K. Diffraction data were recorded over a 180° rotation of the crystal around the φ axis as 360 diffraction images with a width of 0.5° per image. The data were processed using *AUTOMAR* (http://www.marresearch.com/automar/automar/guide.htm).

3. Results and discussion

The mannan endo-1,4-β-mannosidase (β-mannanase) gene (*manB*) from *B. licheniformis* strain DSM13 with a C-terminally attached His_6 tag was expressed in *E. coli* Top10 as described previously (Songsiriritthigul, Buranabanyat *et al.*, 2010). Purification of the recombinant mannanase by Ni–NTA agarose affinity chromatography yielded 50 mg highly purified protein per litre of bacterial culture. Fig. 1 shows eluted fractions from the Ni–NTA agarose column, indicating a highly purified band of apparent molecular weight 41 kDa as determined by SDS–PAGE. The expressed protein exhibited mannanase activity as shown by a gel activity assay using locust bean gum as a substrate. The specific activity of the recombinant enzyme using high-viscosity locust bean gum substrate was 1672 ± 96 U mg^{-1}. MALDI–TOF measurements showed that the recombinant enzyme is monomeric, with a molecular mass of 39 210 Da. These data agree well with the theoretical mass of the mature recombinant enzyme containing a C-terminal His_6 tag (39 243.89 Da), the signal sequence of which was cleaved between Ser22 and Arg23. These two amino acids are from the *Bgl*II cloning site that was used to ligate the mannanase-encoding DNA fragment just after the *E. coli* OmpA signal peptide on the pFLAG-CTS plasmid.

The thermostability of our mannanase is of interest to industry and previous structural and functional studies on *B. subtilis* Z-2 mannanase have revealed that a Zn^{2+} ion bound between His1 at the N-terminus and Glu336 at the C-terminus contributes to stability (Yan *et al.*, 2008). Using synchrotron X-ray fluorescence and fluorescence-yield X-ray absorption near-edge structure, Zn^{2+} and Ni^{2+} were detected in our purified *B. licheniformis* mannanase (data not shown), suggesting that a similar metal-binding site may contribute to its high thermal stability.

The single crystal obtained from streak-seeding was exposed to X-rays using its mother liquor containing 20%(*v*/*v*) glycerol as a cryoprotectant. However, it did not diffract well (~10.4 Å resolution). Streaked diffraction spots to ~2.4 Å resolution were obtained from a crystal optimized from condition 15 of Crystal Screen. Finally, the best crystal was obtained using a reservoir solution consisting of 12%(*w*/*v*) PEG 8000, 0.2 *M* magnesium acetate tetrahydrate in 0.1 *M* MES pH 6.5 with dimensions of 160 × 115 × 15 µm (Fig. 2). It diffracted X-rays to at least 2.3 Å resolution (Fig. 3). This mannanase crystal belonged to a primitive monoclinic space group, which was found to be $P2_1$ based on systematic absences and molecular replacement (see below). The refined unit-cell parameters were a = 48.58, b = 91.75, c = 89.55 Å, β = 98.29° and the crystal contained two molecules per asymmetric unit, with an estimated Matthews

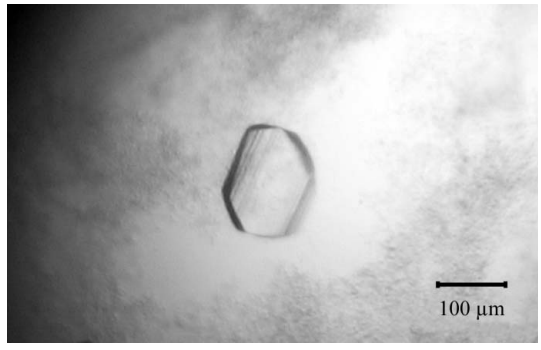

Figure 2
A crystal of β-mannanase with average dimensions of 160 × 115 × 15 µm was obtained from a hanging-drop vapour-diffusion setup using 12%(*w*/*v*) PEG 8000, 0.2 *M* magnesium acetate tetrahydrate in 0.1 *M* MES pH 6.5.

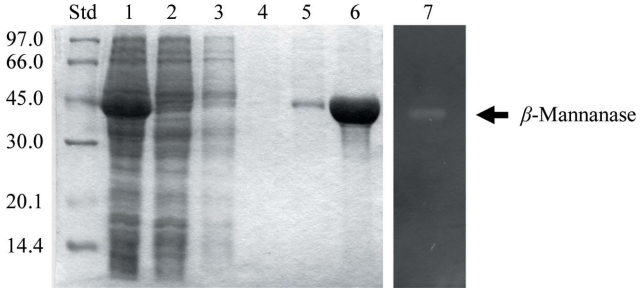

Figure 1
SDS–PAGE and zymogram analysis of purified β-mannanase from *B. licheniformis* DSM13. Lane Std, standard low-molecular-weight protein markers (kDa); lane 1, cleared cell lysate after sonication; lane 2, flowthrough of unbound proteins; lanes 3 and 4, 5 m*M* imidazole wash fractions; lane 5, 20 m*M* imidazole wash fraction; lane 6, fraction eluted with 250 m*M* imidazole; lane 7, purified enzyme shown by in-gel activity staining.

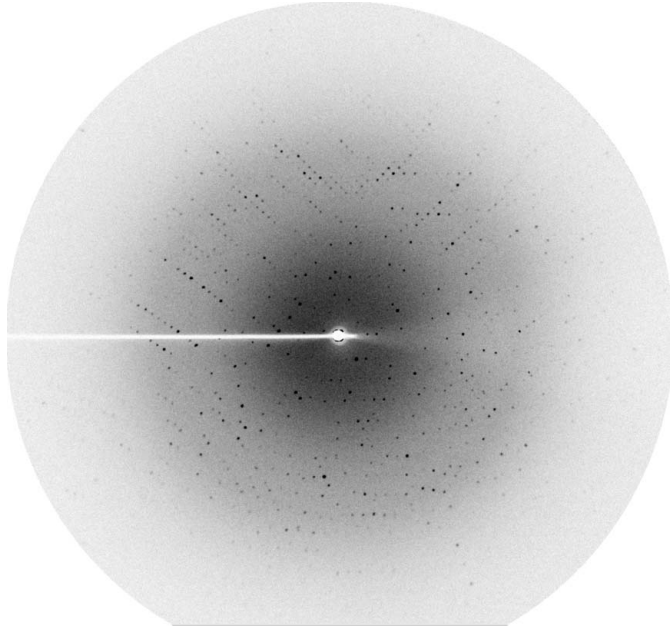

Figure 3
A diffraction image from a mannanase crystal recorded using a rotating-anode source at the Macromolecular Crystallography facility of the Synchrotron Light Research Institute (SLRI), Thailand.

Table 1
Data-collection and structure-solution statistics.

Values in parentheses are for the outer shell.

Space group	$P2_1$
Unit-cell parameters (Å, °)	a = 48.58, b = 91.75, c = 89.55, $\alpha = \gamma = 90$, $\beta = 98.29$
Matthews coefficient V_M (Å^3 Da^{-1})	2.55
Solvent content (%)	51.82
Wavelength (Å)	1.5418
Temperature (K)	100
Resolution range (Å)	27.94–2.30 (2.42–2.30)
No. of unique reflections	34614
No. of observed reflections	121760
Completeness (%)	99.9 (99.7)
Multiplicity	3.5 (3.5)
$\langle I/\sigma(I)\rangle$	12.3 (2.3)
R_{merge}†	11.0 (41.8)

† $R_{merge} = \sum_{hkl}\sum_i |I_i(hkl) - \langle I(hkl)\rangle| / \sum_{hkl}\sum_i I_i(hkl)$, where $I_i(hkl)$ is the intensity of the ith measurement of an equivalent reflection with indices hkl.

coefficient of 2.55 Å^3 Da^{-1} and a solvent content of 51.82% (Matthews, 1968). The statistics of data collection and processing are summarized in Table 1.

A preliminary solution of the structure of β-mannanase from *B. licheniformis* strain DSM13 was obtained by molecular-replacement calculations using the *AMoRe* program (Navaza, 1994) from *CCP*4 (Collaborative Computational Project, Number 4, 1994) with the crystal structure of mannanase from *B. subtilis* Z-2 (PDB code 2qha; 81.90% identity to β-mannanase from *B. licheniformis* strain DSM13; Yan *et al.*, 2008) as the search model. Two molecules were placed per asymmetric unit, giving an amplitude correlation coefficient of 36.4% and an R factor of 47.6%. This confirmed the twofold noncrystallographic symmetry and indicated that the space group was $P2_1$. Examination of the best solution revealed good crystal packing and no clashes between symmetry-related molecules. This preliminary model is currently being rebuilt and refined.

This research was financially supported by the Synchrotron Light Research Institute (grant No. 1-2551/LS02). We would like to thank W. Klysubun and the operators at Beamline 8 of SLRI for technical assistance in XRF and XANES measurements.

References

Akita, M., Takeda, N., Hirasawa, K., Sakai, H., Kawamoto, M., Yamamoto, M., Grant, W. D., Hatada, Y., Ito, S. & Horikoshi, K. (2004). *Acta Cryst.* D**60**, 1490–1492.

Bolam, D. N., Hughes, N., Virden, R., Lakey, J. H., Hazlewood, G. P., Henrissat, B. & Gilbert, H. J. (1996). *Biochemistry*, **35**, 16195–16204.

Bourgault, R., Oakley, A. J., Bewley, J. D. & Wilce, M. C. (2005). *Protein Sci.* **14**, 1233–1241.

Bradford, M. M. (1976). *Anal. Biochem.* **72**, 248–254.

Cantarel, B. L., Coutinho, P. M., Rancurel, C., Bernard, T., Lombard, V. & Henrissat, B. (2009). *Nucleic Acids Res.* **37**, 233–238.

Chitnumsub, P., Yavaniyama, J., Vanichtanankul, J., Kamchonwongpaisan, S., Walkinshaw, M. D. & Yuthavong, Y. (2004). *Acta Cryst.* D**60**, 780–783.

Collaborative Computational Project, Number 4 (1994). *Acta Cryst.* D**50**, 760–763.

Dhawan, S. & Kaur, J. (2007). *Crit. Rev. Biotechnol.* **27**, 197–216.

Ducros, V. M.-A., Zechel, D. L., Murshudov, G. N., Gilbert, H. J., Szabó, L., Stoll, D., Withers, S. G. & Davies, G. J. (2002). *Angew. Chem. Int. Ed.* **41**, 2824–2827.

Harjunp, V., Teleman, A., Siika-Aho, M. & Drakenberg, T. (1995). *Eur. J. Biochem.* **234**, 278–283.

Henrissat, B. (1991). *Biochem. J.* **280**, 309–316.

Henrissat, B. & Davies, G. (1997). *Curr. Opin. Struct. Biol.* **7**, 637–644.

Hilge, M., Gloor, S. M., Rypniewski, W., Sauer, O., Heightman, T. D., Zimmerman, W., Winterhalter, K. & Piontek, K. (1998). *Structure*, **6**, 1433–1444.

Hogg, D., Woo, E. J., Bolam, D. N., McKie, V. A., Gilbert, H. J. & Pickersgill, R. W. (2001). *J. Biol. Chem.* **276**, 31186–31192.

Koshland, D. E. (1953). *Biol. Rev. Camb. Philos. Soc.* **28**, 416–436.

Laemmli, U. K. (1970). *Nature (London)*, **227**, 680–685.

Larsson, A. M., Anderson, L., Xu, B., Muñoz, I. G., Usón, I., Janson, J.-C., Stålbrand, H. & Ståhlberg, J. (2006). *J. Mol. Biol.* **357**, 1500–1510.

Le Nours, J., Anderson, L., Stoll, D., Stålbrand, H. & Lo Leggio, L. (2005). *Biochemistry*, **44**, 12700–12708.

Matthews, B. W. (1968). *J. Mol. Biol.* **33**, 491–497.

McCleary, B. V. (1988). *Methods Enzymol.* **160**, 596–610.

Moreira, L. R. S. & Filho, E. X. F. (2008). *Appl. Microbiol. Biotechnol.* **79**, 165–178.

Navaza, J. (1994). *Acta Cryst.* A**50**, 157–163.

Sabini, E., Schubert, H., Murshudov, G., Wilson, K. S., Siika-Aho, M. & Penttilä, M. (2000). *Acta Cryst.* D**56**, 3–13.

Schallmey, M., Singh, A. & Ward, O. P. (2004). *Can. J. Microbiol.* **50**, 1–17.

Songsiriritthigul, C., Buranabanyat, B., Haltrich, D. & Yamabhai, M. (2010). *Microb. Cell Fact.*, doi:10.1186/1475-2859-9-20.

Songsiriritthigul, C., Lapboonrueng, S., Pechsrichuang, P., Pesatcha, P. & Yamabhai, M. (2010). *Bioresour. Technol.* **101**, 4096–4103.

Songsiriritthigul, C., Pesatcha, P., Eijsink, G. H. V. & Yamabhai, M. (2009). *J. Biotechnol.* **4**, 501–509.

Veith, B., Herzberg, C., Steckel, S., Feesche, J., Maurer, K. H., Ehrenreich, P., Baumer, S., Henne, A., Liesegang, H., Merkl, R., Ehrenreich, A. & Gottschalk, G. (2004). *J. Mol. Microbiol. Biotechnol.* **7**, 204–211.

Yamabhai, M., Buranabanyat, B., Jaruseranee, N. & Songsiriritthigul, C. (2011). In the press.

Yamabhai, M., Emrat, S., Sukasem, S., Pesatcha, P., Jaruseranee, N. & Buranabanyat, B. (2008). *J. Biotechnol.* **133**, 50–57.

Yan, X.-X., An, X.-M., Gui, L.-L. & Liang, D.-C. (2008). *J. Mol. Biol.* **379**, 535–544.